

Version date: 2023-01-26

Responsible: Petri Niemelä

Document name: FS1 ADCS PSD Sun Sensor Design Document

Foresail-1

**PSD Sun Sensor Design
Document**

Aalto University

Department of Electronics and Nanoengineering

PSD Sun Sensor Design Document

FS1 ADCS PSD Sun Sensor Design Document

Responsible: Petri Niemelä

Version date: 2023-01-26

Page: 2 / 22

Authors

Name	Worked with parts
Petri Niemelä	The whole document

Approved by

Table of Contents

1 General	4
1.1 Scope	4
1.2 Applicable Documents	4
1.3 Reference documents	4
1.4 Abbreviations and acronyms	4
2 Sensor Design	5
2.1 Performance	6
2.2 Sun vector estimation	9
3 Electrical Design	10
3.1 Electrical Interface	10
3.2 Microcontroller	10
3.2.1 Radiation Hardening	11
3.3 Transimpedance Amplifiers	11
3.4 Analog Digital Converter	14
3.5 Power supply	14
3.6 I2C bus isolation	14
3.7 Operating environment	15
4 Mechanical Design	16
4.1 Mechanical Interface	16
5 Digital interface	17
5.1 I2C Commanding Protocol	17
5.2 RS-485 Commanding Protocol	17
5.3 Command set	17
6 References and further reading	19
7 Appendices	21
7.1 Schematics	21
7.2 Bill of Material	21
7.3 PCB layout	22

1 General

1.1 Scope

This document represents a detailed design of the PSD Sun Sensor designed for FORESAIL-satellites. This document applies for **hardware version v3 (I2C variant) and v4 (RS-485 variant)**.

The public design files can be found from Github-repository:

https://github.com/foresail/fs1_psd_sun_sensor

1.2 Applicable Documents

[AD-01] [FS1 ADCS PSD Sun Sensor Prototype Test Plan](#)

[AD-02] [FS1 ADCS PSD Sun Sensor Qualification Test Report template](#)

1.3 Reference documents

[RD-01] Hamamatsu S5990-01 Two-Dimensional PSD

datasheet: https://www.hamamatsu.com/resources/pdf/ssd/s5990-01_etc_kpsd1010e.pdf

[RD-02] Texas Instrument's MSP430FR231x Mixed-Signal Microcontrollers

datasheet: <http://www.ti.com/lit/ds/slase58d/slase58d.pdf>

[RD-03] Texas Instrument's OPAx340 Single-Supply, Rail-to-Rail Operational Amplifiers

datasheet: <http://www.ti.com/lit/ds/symlink/opa4340.pdf>

1.4 Abbreviations and acronyms

ADC	Analog-to-Digital Converter
FRAM	Ferroelectric Random Access Memory
FOV	Field Of View
MCU	Microcontroller
PCB	Printed Circuit Board
PSD	Position Sensitive Detector/Device
TIA	Transimpedance Amplifier
WDT	Watchdog Timer

2 Sensor Design

The PSD sensor (Position Sensitive Detector/Device/Diode) is a light sensitive photodiode which produces a small current when exposed to light. The PSD differs from the normal photodiode by having four cathodes and one anode for one single large detector area. When the sensitive area is illuminated with a relatively small spot of light the produced currents are distributed depending on the position of the light spot. When the light spot is created using a pinhole structure the sensor can be used to measure direction/angle of the incoming light and thus the concept can be applied for making a sun sensor.

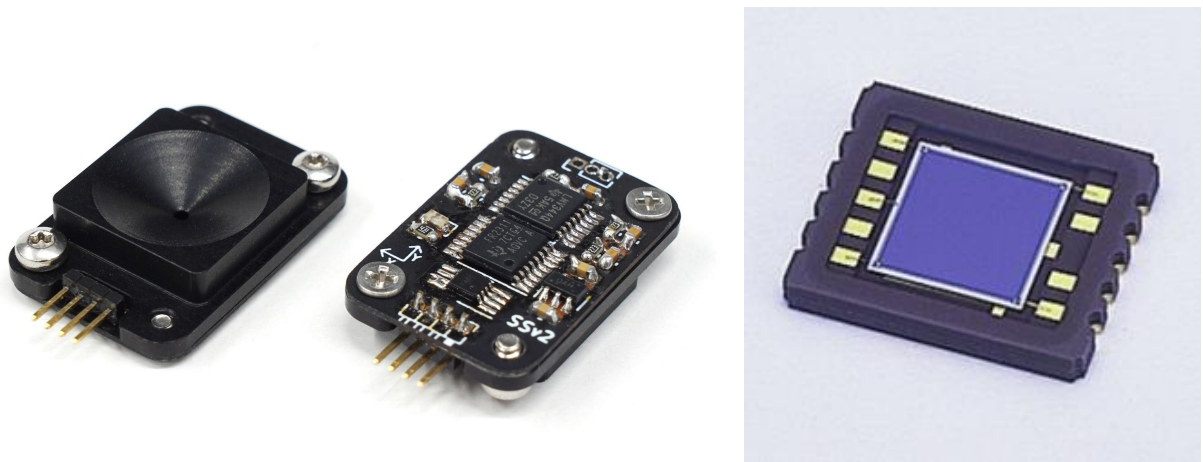


Figure 1: PSD Sun Sensor version 2 and Hamamatsu S5990-01 Position Sensitive Device

The used PSD, **Hamamatsu S5990-1**, (In Figure 1) is so called tetra-lateral type (pin-cushion type) that delivers improved position detection and linearity compared to other similar diodes. The sensor has a large 4×4 mm active area. [RD-01]

PSD sensors advantages in sun sensor application can be considered: simple electrical and mechanical design and easily achievable large Field of View (FOV). The sensor design's largest disadvantage is its sensitivity for straylight meaning that the sensor cannot discriminate between direct sunlight and reflected sunlight. Reflections, for example from moonshine or earthshine, cause bias error which cannot be easily eliminated from the measurements. Effect of this will be discussed later in detail.

The general characteristics of sensor design are:

- Dimensions: 24 mm \times 16 mm \times 6 mm
- Mass: 4 grams
- Panel mountable into 14x14 mm hole with two M2 screws
 - Extension behind the panel: 3.1 mm
- Electrical connection by soldering on the panel PCB or by harness.
- FOV: \sim 100 degrees, resolution: 0.13° , accuracy: $\pm 1^\circ$ (discussed in the following sections)
- Refresh rate up to 100 Hz. (Sampling time: 4 ms + communication overhead)
- Can provide following data products:
 - Raw current measurements
 - Point & intensity measurements
 - Sun vector & intensity measurements
 - Angles & intensity measurements

- I²C digital serial interface (applicable for hardware version 3)
 - Maximum bus speed 400 kHz at 3.3V logic level.
 - I²C address can be configured via the command interface.
 - The I²C bus is isolated when the sensor is unpowered.
- RS-485 digital interface (applicable for hardware version 4)
 - Follows reduced Foresail multi-drop RS-485 protocol definition
 - TBD
- Low power consumption < 4 mW
 - Sleep: 0.45 mA @3.6 V
 - Sampling: 0.9 mA @3.6 V
 - Peak sampling: TBD mA @3.6V
 - In-rush current: TBD mA @3.6V
- Operating voltage: 2.0 – 5.5 V
 - The standard version has a 3.3V LDO and designed operating voltage is around 3.6V.
 - MSP430 can operate with voltages down to 1.8 V.

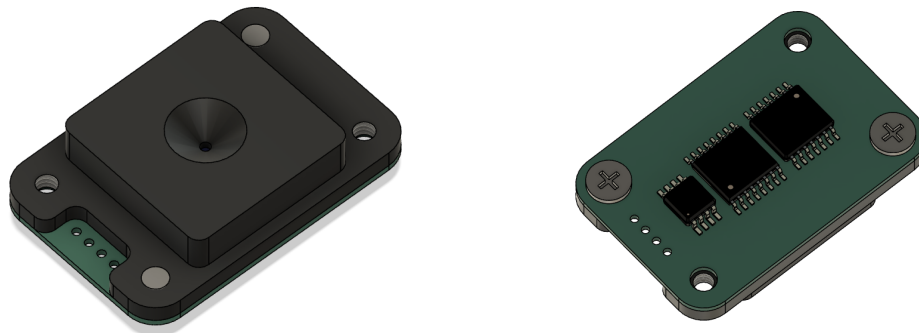


Figure 2: Front and back side of the PSD Sun Sensor assembly from CAD program.

2.1 Performance

The performance (FOV and accuracy) of the sensor is mainly determined by the geometry of the pinhole structure. The pinhole geometry is illustrated in the following figure. By adjusting the distance of the pinhole from the sensor. On the Foresail-1 PSD Sun Sensor the distance from photodiode to pin hole is 1.50 mm.

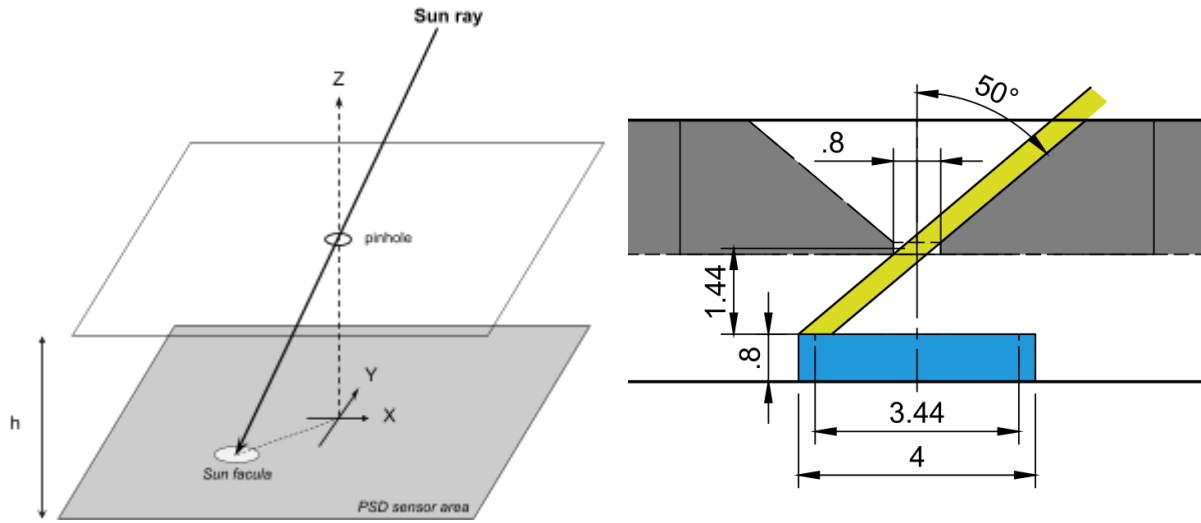


Figure 3: On left the sensor's pinhole geometry illustrated in 3D. On the right the sensor's actual pin hole geometry with dimensioning.

Field of View:

The maximum field of view of the sensor is determined by its

$$\tan(FoV/2) = \frac{0.5 \cdot (w - d)}{h} = \frac{0.5 \cdot 3.44 \text{ mm}}{1.44 \text{ mm}} \Rightarrow FoV = 100^\circ$$

In practice the sensor has an even larger FOV. (see calibration results)

Resolution:

When using 10 bits (1024 counts) per channel and because there are two channels per axis, each axis is "sampled" in 11-bit resolution. Thus, at the center of the sensor the theoretical resolution is:

$$\theta = \operatorname{atan}\left(\frac{(3.44 \text{ mm} / 1024)}{1.44 \text{ mm}}\right) \simeq 0.134^\circ$$

This resolution improves when moving toward the edge of the sensor. Smaller angle changes in the Sun direction causes larger changes in light spot position. At the edge the theoretical resolution is:

$$\theta = \operatorname{atan}\left(\frac{0.5 \cdot 3.44 \text{ mm}}{1.44 \text{ mm}}\right) - \operatorname{atan}\left(\frac{0.5 \cdot 3.44 \text{ mm} \cdot 511/512}{1.44 \text{ mm}}\right) \simeq 0.055^\circ$$

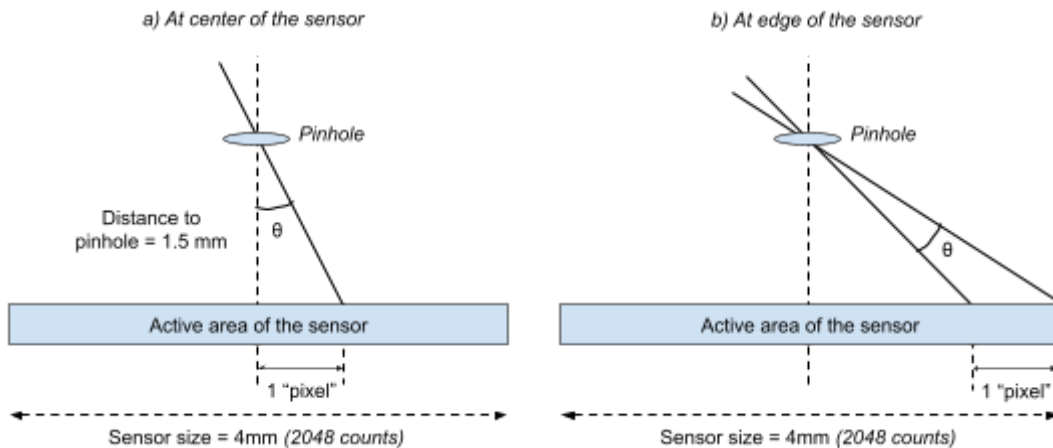


Figure 4: Resolution estimated using simplified pin hole geometry.

In theory, the resolution doesn't depend on the size of the light spot until the light spot is clipped by

the edge of the active area of the sensor. The output currents and the current distribution depends on the intensity of the light and the “mass center” of the light. If the light spot size is increased its mass center stays the same. Only the intensity (amount of light passing through the pinhole) changes. The sensor’s gain can be adjusted using for any pinhole

Real accuracy:

In theory the sensor could achieve better than 0.15° accuracy but in practice the accuracy is not that good and it is affected by numerous error sources. In this section some of those error sources are analyzed. In practice the resolution of PSD based sensors varies between around $1 - 5^\circ$. If someone claims better accuracy (with similar FOV and single sensor) than this when using the same sensor technology, they most likely lie or don't tell the whole truth.

Error sources:

- 1) The sensor cannot differentiate between different sources of light: Sun, moon, Earth’s Albedo, specular reflections from the Earth’s surface. Discussed in detail in the next section.
- 2) The pinhole structure is not a perfect pinhole. Incoming light can reflect from the edge hole and cast a second light spot. Black anodisation aims to cope with this problem.
- 3) At high angles the cover glass can refract the light spot. This effect can be partially calibrated.
- 4) The light spot can reflect from the cover glass and bounce inside the sensor. The error caused by the reflections inside the sensors are tried to minimize by anodizing the sensor cover black.
- 5) The response of the PSD is not completely linear aka current distribution doesn’t map the light spot position perfectly. This happens both in axis and diagonally mapping. Hamamatsu’s tetra-lateral type (pin-cushion type) PSD aims to compensate for this.
- 6) The ADC is not perfect and it has noise on its results. According to the MCU’s datasheet ADC Effective error in 10-bit mode is ± 2 LSB (least significant bits). Based on this the accuracy is less than 0.3° . ADC noise could be reduced by using oversampling because the sampling noise is gaussian by its nature. This is not seen beneficial because other error sources are more dominant and multi-sampling would just slow down the sampling.
- 7) Thermal expansion of the components is not considered. The surface temperature of the satellite can vary between -40°C and 40°C . The sensor cover should have a mirror finish on its front side to minimize heat load.
- 8) Sensor mounting on the satellite structure easily introduces a significant systematic error which is larger than the accuracy of the sensor. Calibrating the sensor position/orientation relative to the satellite’s coordinate system should be performed after final assembly but such test setup is not simple.

Effect of the straylight:

PSD sun sensor's greatest disadvantage is its incapability to differentiate between different light sources. The currents generated by different light sources (Sun, Earth, Moon shine and specular reflections from Earth’s surface) sums up together and cannot be separated from each other. Thus, Earth’s and Moon’s albedos add a bias error into Sun direction estimation if they are visible at the same time. Because each satellite’s face has a dedicated sun sensor and only the strongest signal is taken into consideration in sun vector determination, the Earth’s albedo affects the sun vector measurements only when the Sun and Earth are inside the same 90° FOV “pyramide”. This happens

when the satellite is above 66° latitude (north or south) and $\pm 24^\circ$ around the termination zone. The influence of Earth's albedo is constantly on sun synchronous orbit, which Mean Local Time of the Ascending Node (LTAN) is between 04:24 - 08:36 and 16:36 - 19:24. These regions are illustrated in the Figure 5.

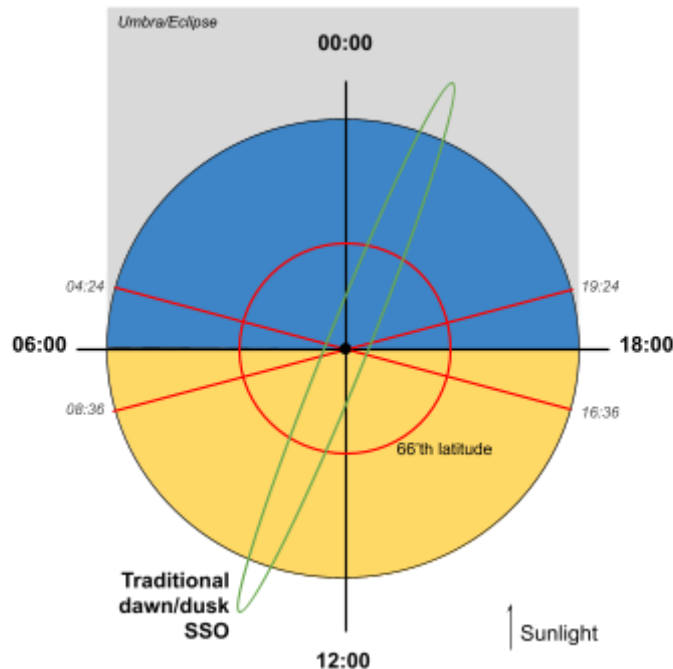


Figure 5: Orbit regions where PSD's operation is affected by Earth's albedo.

The effect of Earth's albedo to the accuracy of PSD sun sensor is greatly discussed in Robert Valner's bachelor's thesis: http://dspace.ut.ee/bitstream/handle/10062/30981/Robert_Valner.pdf In his thesis he concludes that: "the net uncertainty of the measurements of the sensor is 2.5° with coverage probability of approximately 95%"

Intensity accuracy:

The intensity measurement of the sensor is relative and should not be used as absolute measurement. The sensor's intensity output is the average of each channel's output in range from 0 to 1024. The reading highly depends on the sensor's temperature due to photodiodes efficiency characteristics and temperature drift of the voltage reference.

The intensity reading itself could be also used to determine the sun angle using inverse cosine law and with temperature compensation using the MCU's temperature sensor could provide better absolute accuracy but this is implemented because it's not seen beneficial for an attitude control system as whole. The linearity of the intensity measurement is not known.

What could be improved?

Possible methods to improvement accuracy:

1. More sensors with smaller FOV
2. Add UV bandpass filter to remove the effect of albedo and specular reflections.

2.2 Sun vector estimation

The determination of the sun vector from multiple sun sensors can be done using following simple algorithm:

```
meas = get_all_sun_vectors()

sun_detected = false
sensor_i = arg_max(meas.intensity)
if meas[sensor_i].intensity > detection_threshold:
    sun_direction = apply_rotation(sensor_i, meas[sensor_i].vector)
    sun_detected = true
```

3 Electrical Design

The electrical design of the sensor is very simple. It consists of a PSD sensor itself (aka four channel photodiode), four transimpedance amplifiers and a MCU for analog to digital conversion and digital communication.

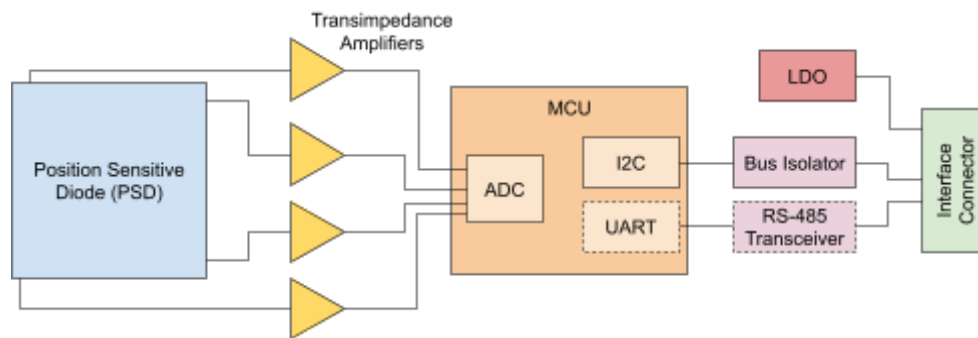


Figure: Block diagram of the sensor's electrical components and their connections.

3.1 Electrical Interface

The sensor's electrical interface is described in the table below.

Table: Sensor pinout

Pin number	Pin name on version 3	Pin name on version 4
1	GND	GND
2	VCC	VCC
3	I2C SDA	RS-485 DATA+
4	I2C SCL	RS-485 DATA-

On the PCB the electrical connection is done to the 1.27 mm pitch pin 4 hole connector footprint. To this footprint the electrical connection can be done by directly soldering the sensor on a PCB panel using a right angle 1.27mm pin header or by soldering a pigtail cable on it.

3.2 Microcontroller

The PSD sun sensors' MCU is Texas Instrument's MSP430FR2311IPW16. MCU's important features are: [RD-02]

- Small TSSOP-16 package
- Runs at 4 MHz
- 3.75KB of Program **FRAM** (Radiation Resistant and Nonmagnetic) + 1KB of RAM
- Internal 1.2V voltage reference
- 8 channel **10-Bit Analog-to-Digital Converter** (ADC) with internal 1.5V voltage reference
- Optimized low **power modes** (32nA in shutdown)
- Wide support for serial communication protocols such as **I²C**, **UART** etc.
- Internal brown-out detection circuit

The selected MCU has also internal opamp which could have been used for something.

3.2.1 Radiation Hardening

Following radiation hardening are considered in the design:

1. Usage of system FRAM memory:

The selected MCU uses FRAM technology for storing its firmware. The FRAM technology is known from its radiation hardness on a memory cell (SEU: Single Event Upsets). This doesn't ensure complete radiation hardness against other types of single events. Single events can also happen in the memory controllers etc.

Also the sensor is vulnerable to destructive single events burnouts if no latching.

The dose tolerance of the MCU is not known and it could be generalized outside of a single batch.

2. Watchdog Timer:

Watchdog resets the MCU every ~40 seconds if the main loop stops running. Heartbeat timer tries to wake up the processor every 70 ms to execute the main loop.

3. Register refreshing by resetting:

Sensor initializes itself every 2 minutes in nominal state to refresh all internal peripheral registers.

3. Component-level power cycling:

The opamp's power is supplied from MCU's IO-pin which works as current limiter and load switch and it can be used to cycle on every reset.

4. Sensor Aluminium shielding

At the surface of the satellite, the sensor experiences a harsher radiation environment compared to the rest of the electronics on board inside the radiation shielding. To compensate this a little bit, the thickness of the aluminum sensor cover has not been minimized to give some protection against total dose effects. The only way to improve this more is to move the electronics beside the PSD photodiode itself inside the satellite.

3.3 Transimpedance Amplifiers

For PSD sensor current measurement the sensor board has **four transimpedance amplifiers (TIA)** to perform current-voltage conversion with predefined gain. The amplifier gain is set by the external resistor and adjusted depending on illumination levels, hole size etc. Photodiodes are in zero reverse bias configuration for improved sensitivity at low intensities. Additionally, a filtering capacitor is placed parallel on the feedback loop to cut-off frequencies above 100 Hz.

When the current is zero the opamp outputs the reference voltage and higher the current lower the output voltage is. The output voltage can be then measured by the ADC. MSP430's internal voltage reference (VREF+) is used for the opamp. The precision of the voltage reference doesn't affect the overall point position measurements. The possible reference voltage drift affects only absolute intensity measurements and is the same for all the channels. The point position is calculated from the differences of absolute current measurement as defined in equation X, and thus, possible reference voltage drift won't affect sun vector accuracy. The absolute illumination is not sure for sun vector determination. Also, the diode's leakage current will vary based on the temperature.

On hardware version 4 (RS-485 variant), the MSP430's internal voltage reference cannot be used due to pin mapping collision with an UART pin required for RS-485 transceiver. Thus, an external voltage reference is required for the opamps. There are no real requirements for the reference other than voltage should be such that the opamp doesn't need to drive till the rail voltage. Absolute stability is not required because the intensity measurements are already relative by their nature and the reference is shared between the channels. Also the voltage reference is connected to very high impedance (only opamps inputs), so the current draw is negligible. Thus, to keep the BOM and PCB layout simple a simple 1:1 resistor divider was chosen to generate 1.65 V reference. The resistor divider as voltage reference is sensitive for source voltage but in this case the 3.3V source voltage is regulated very close to the divider itself.

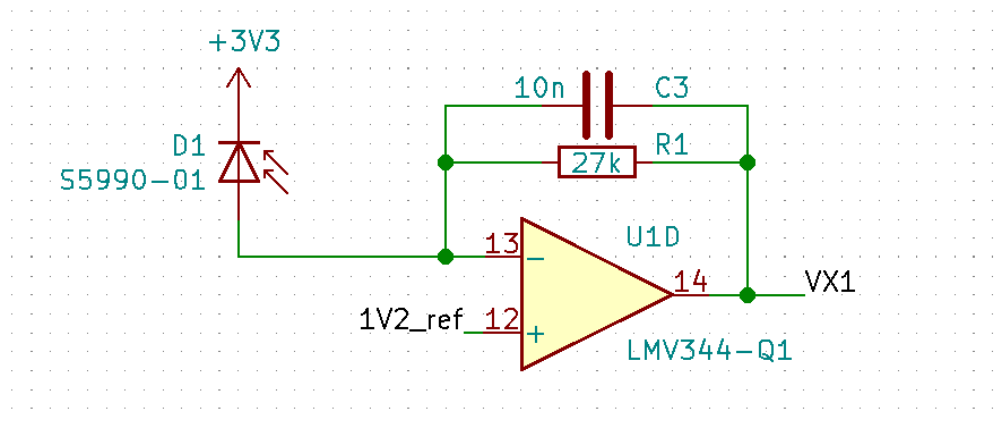


Figure 6: Simplified circuit diagram of a transimpedance amplifier.

The chosen operational amplifier is automotive quality **LMV344-Q1** quad rail-to-rail output CMOS operational amplifier in small TSSOP-14 package [RD-03]. The opamp has relatively narrow bandwidth (1 MHz), low power consumption 100 μ A (typical). Measured current consumption in dark: **230 μ A**. (0.83 mW @3.6 V)

Opamp's positive rail is at 3.3 V and negative at GND. The opamp is powered from MCU's GPIO pin thus can be turned to save even more power. This is possible due to the low power consumption of the opamp.

The response of the transimpedance amplifier circuit was simulated using LTspice simulation program. The simulation model is illustrated in Figure 7. The model was used to confirm the AC response of the filter (Figure 8). Also, an input waveform for the photodiode current source was generated using a simple Python script. The amplifier circuit's time domain response when attach on a satellite spinning at 1 Hz can be seen in Figure 9.

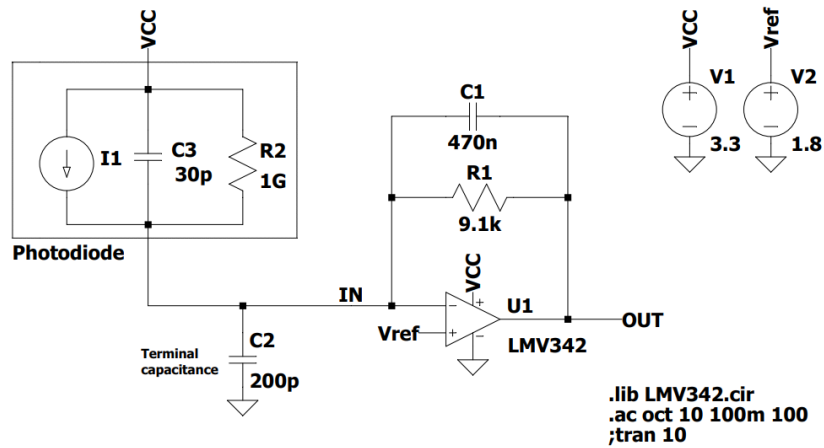


Figure 7: LTSpice model used to simulate the transimpedance amplifier transient and AC responses. (The used LMV342 opamp is identical LMV344 but has different number of channels)

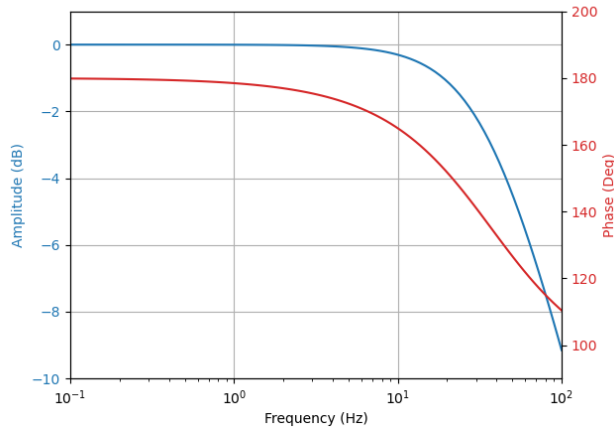


Figure 8: The AC response of the transimpedance filter. The -3dB cutoff frequency is around 37 Hz.

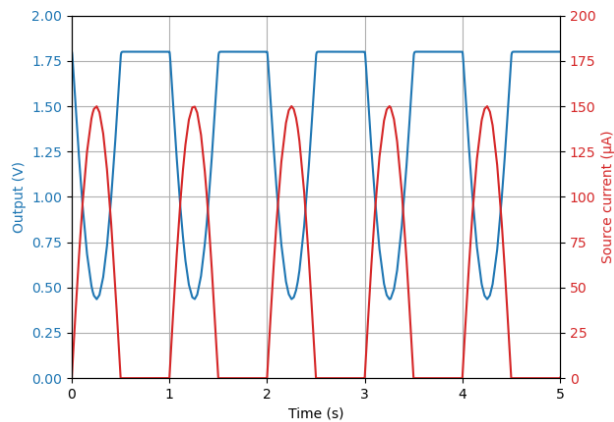


Figure 8: Transient response of the TIA for 1Hz (60 rpm) spin. The output voltage response is inverted compared to the produced current of the photodiode due to the reverse bias design. Small amount of smoothening can be seen on the trailing edge due to low pass filtering.

3.4 Analog Digital Converter

The analog to digital conversion is done using MSP430's internal 8-channel 10-bit ADC and the analog lines are referenced against MSP430's 1.2 V reference (VREF+) which is externally connected to ADC's VREF+ -pin.

The ADC samples the different voltage channels in sequence and not simultaneously. The small sample time difference is considered to be negligible for the precision of the sensor. For a satellite spinning at 1 Hz, the satellite attitude changes 1.1° during the 3 ms sampling time.

Temperature sensor: MSP430 has an internal temperature sensor which is connected to ADC's channel 12. Temperature sensor voltage is compared to ADC's internal 1.5 V reference. The maximum temperature the sensor can measure is roughly 170°C . Above this temperature the sensor voltage goes above 1.5 V.

ADC count to temperature is thus coefficient:

$$3.35 \text{ mV}/^\circ\text{C} \Rightarrow (1500\text{mV} / 1024 \text{ counts}) / 3.35\text{mV}/^\circ\text{C} = 4.37^\circ \text{ dC}/\text{count}$$

Equation on the MCU:

$$T(^{\circ}\text{dC}) = (\text{ADCcount} - \text{calib}) / 4^{\circ}\text{dC}/\text{count} + 300^{\circ}\text{dC}$$

3.5 Power supply

The sensor is designed to take 3.6 V input voltage and has 3.3 V low dropout voltage (LDO) regulator on board. Lower voltages are possible down to 2.5V with the same opamp or down to 1.5 V the opamp is changed to a similar kind of with lower input voltage rating. The LDO can be also bypassed with a 0-ohm resistor if wanted.

3.6 I²C bus isolation

Sun sensor uses SN74TVC3306 bus level translation IC as I²C bus isolator to prevent stalling the I²C bus when the sensor is not powered. The isolator also prevents the sensor from being powered via the SDA/SCL lines due to low power consumption of the MSP430 processor. The isolator IC is basically three individual NMOS transistors (also called dual voltage clamp) and can be considered robust design for higher radiation environment. The down side of this type of isolator is the 3.5 ohm high-ish series resistance.

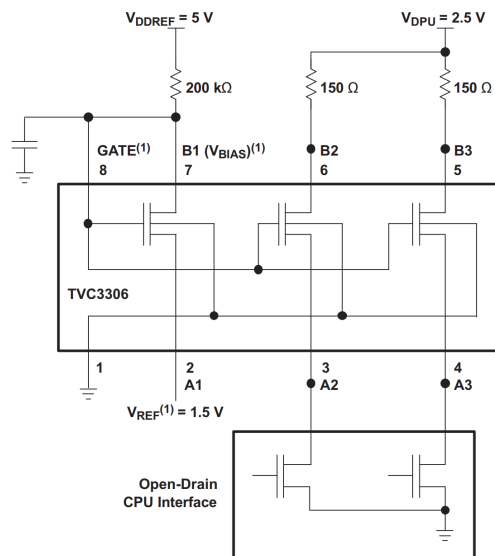


Figure 9: Internals of the SN74TVC3306 IC used for the I2C bus

3.7 Operating environment

The PSD sun sensors are expected to encounter large temperature variations in the low earth orbit conditions on the surface of the satellite. On the surface of the satellite, sensors are exposed to direct sunlight and cold space in turns with very little thermal inertial and poor thermal conduction to the rest of the satellite's structure. It has been estimated that the surface temperatures of the cubesat in LEO will at least vary from -20 to 30 °C on every orbit and in the worst case -40°C to 60°C.

The recommended operating temperature ranges for each component can be seen in the following table. The most limiting recommended temperature range is for Hamamatsu's PSD diode whose lower temperature limit is -20°C. Low temperatures doesn't inherently degrade the electrical performance of a diode but the diode's packaging method might be the reason for the lowered rating. (Maybe the manufacturer hasn't just performed the qualification test for lower temperatures.) There are no huge concerns to suspect that the diode would fail right after -20°C. Also, thermal vacuum verification tests with -40 to +100°C temperature range are performed for all the PSD sun sensors assemblies at subsystem level.

Table: Off-the-self component environment ratings

Component	Recommended Operating Temperature
Hamamatsu S5990-01	-20°C to +60°C
MSP430FR2311IPW16	-40°C to +80°C
LMV344-Q1	-40°C to +125°C
TLV71333P-Q1	-40°C to +125°C
SN74TVC3306	-40°C to +80°C

The sensor PCBs are ordered with higher Epoxy glass transition temperature ($T_g=170-180^{\circ}\text{C}$) to make sure the PCB can tolerate high temperature cycles and won't fracture or de-laminate due to material expansion.

Note: A single case of sensor stopping working at temperatures higher than 50°C has been observed. The root cause of the problem was never investigated but it was clearly an analog side failure. The sensor recovered by itself when the temperature decreased below 50°C .

4 Mechanical Design

Sensor's main structural component is the aluminum sensor cover which also works as the pin hole structure for the photodiode. The 0.5mm thick back PCB attaches to the sensor cover using two M2x2 screws and the whole assembly has been designed to be mounted on the panel (Aluminum plate or PCB).

The sensor cover has four M2 threaded holes in total. Two of these are used for attaching the PCB to the cover and other two are used to attach the whole assembly to the panel. Mounting to the panel can be done for example with two M2x4 screws. In Figure 10 the sensor's overall dimensions and the locations of the attachment holes can be seen.

Either of the diagonals can be used for attaching the PCB and for sensor mounting. See preferred from Figures 1 and 2.

4.1 Mechanical Interface

The sensor's mechanical interface can be seen in the figure below.

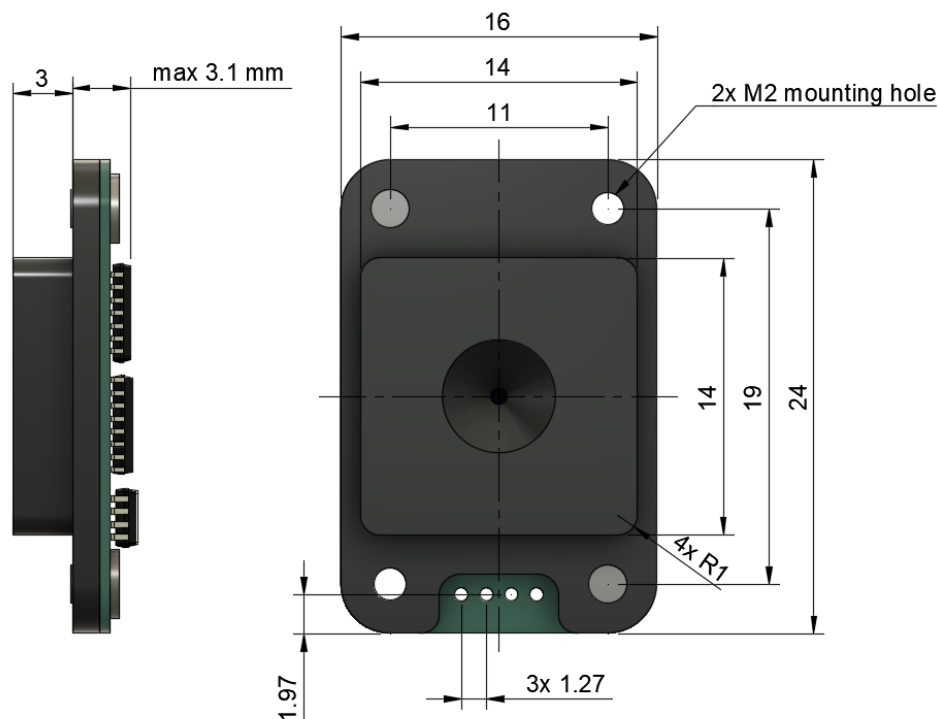


Figure 10: Required panel cut out for the module. The preferred holes for panel mounting are top-right and bottom-left holes.

The sensor is designed to be mounted on a 14x14mm size rectangular hole whose corner has 1mm rounding.

Note: Due to the small size of the sun sensor, the mounting/remounting accuracy of the sensor is not very high. Thus, the sensor's relative orientation to the satellite's reference frame should be calibrated after the final integration.

5 Digital interface

This section defines the I²C and RS-485 digital interfaces and the command set over the bus.

5.1 I²C Commanding Protocol

Sensor's digital interface uses the I²C protocol where the sensor works as a slave. **Default I²C address is 0x6A** and the slave address can be set when reprogramming the sensor or using the I²C commands. Sensor implements a simple I²C protocol which follows the standard I²C data structure and defines the first transmitted byte as a command byte which identifies the command or the response. The protocol commanding and response structure are illustrated in Figure 6.

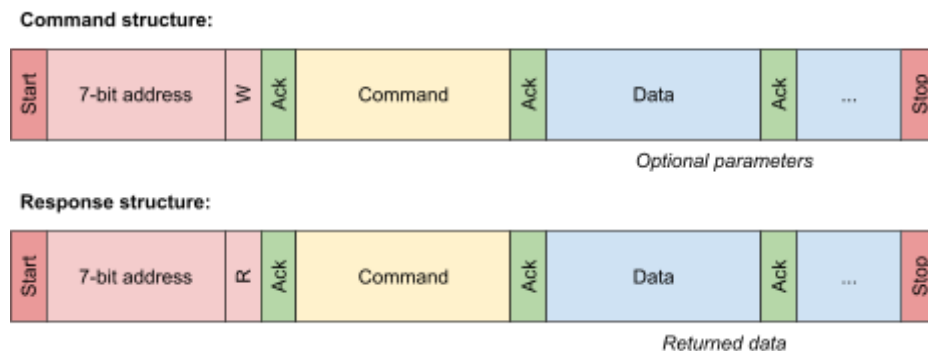


Figure 11: I²C command and response structures

Remarks:

- The default address range for the sensors is: 0x4A - 0x4F
- If the I²C master tries to read the response before the sensor is ready the slave will answer by sending 0xFF.

5.2 RS-485 Commanding Protocol

TBD

5.3 Command set

List of PSD Sun Sensor commands and their functionalities

Remarks:

- Commands which do not return a special data structure return a status code with status command code (0x01).
- All the multi byte integers are in **little endian** format (most significant byte is last).

- If there is no I²C communication on the bus in 2 seconds the MCU will turn off the opamp, voltage references and ADC to save power and unbiased the analog components.

0x01: Status

Read len: 1

Returns response code RSP_OK (0xF0) or RSP_SLEEP (0xF1).

0x03: Get Raw

Runs measurement sequence and returns raw current readings.

Read len: 9

```
typedef struct { // size() = 8 bytes
    uint16_t vx1; // Range: 0 - 1024
    uint16_t vx2; // Range: 0 - 1024
    uint16_t vy1; // Range: 0 - 1024
    uint16_t vy2; // Range: 0 - 1024
} raw_measurements_t;
```

0x04: Get Position

Runs measurement sequence and returns measured light spot position and intensity.

```
typedef struct { // size() = 6 bytes
    int16_t x; // -1024 - +1024
    int16_t y; // -1014 - +1024
    uint16_t intensity;
} position_measurement_t;
```

0x05: Get Angles

Runs measurement sequence and returns measured angles and intensity.

```
typedef struct { // size() = 6 bytes
    int16_t ax; // Desidegrees
    int16_t ay;
    uint16_t intensity;
} angle_measurement_t;
```

Note: The command uses 128 items look-up table and linear interpolation for angle calculation.

0x06: Get Vector

Runs measurement sequence and returns measured sun vector and intensity.

```
typedef struct { // size() = 8 bytes
    int16_t x, y, z;
    uint16_t intensity;
} vector_measurement_t;
```

Note: The reported vector is a direction vector toward the Sun aka signs of the X and Y point positions have been flipped.

0x07: Get All

Runs measurement sequence and returns all three data types listed above (raw, position, angles)
Generally used for testing and verification purposes.

Read len: 21

0x08: Get Temperature

Return MCU temperature as 16-bit signed integer in desi-celsiuses aka $23.5^{\circ}\text{C} = 235$. Read len: 3
Sampling the temperature takes **1.54ms!**

Note: If the temperature calibration offset is set to 0. This function will return the raw ADC count.

0x10: Set Calibration

Set calibration structure.

```
typedef struct {
    int16_t offset_x, offset_y;
    int16_t height;
    int16_t samples;
    int16_t temperature_offset;
} calibration_t;
```

0x11: Get Calibration

Returns the same calibration structure as described for “Set Calibration” command.

Read len: 11

0x12: Set LUT

Set angle look up table values.

TBC

0xE8: Set I2C Address

Set a new I2C address for the sensor. To be applied a power cycling is required.

Note: Exact sampling time of sensor depends on the temperature due to temperar

6 References and further reading

References outside of the project:

1. P. Rodrigues, P. Ramos, “*Design and characterization of A sun sensor for the SSETI-ESEO project*”
<http://citeseerx.ist.psu.edu/viewdoc/download?doi=10.1.1.515.3785&rep=rep1&type=pdf>
2. C. Avsar, J. Lieb, W. Frese, M. Herfort, and S. Trowitzsch, “*Verification of a new two-dimensional sun sensor with digital interface on a sounding rocket.*”
http://rexusbexus.net/wp-content/uploads/2015/06/tupex-3_sse_symposium_paper_expert_panel_version.pdf
3. L. Lin, Z. Sitong, T. Luyang, W. Dong, “*Sun sensor design and test of a micro satellite*”,
<https://www.jvejournals.com/article/17518>
4. D. Faizullin, K. Hiraki, HORYU-IV team, M. Cho, “*Optimization of a Sun Vector Determination for Pinhole Type Sun Sensor*”,

PSD Sun Sensor Design Document

FS1 ADCS PSD Sun Sensor Design Document

Responsible: Petri Niemelä

Version date: 2023-01-26

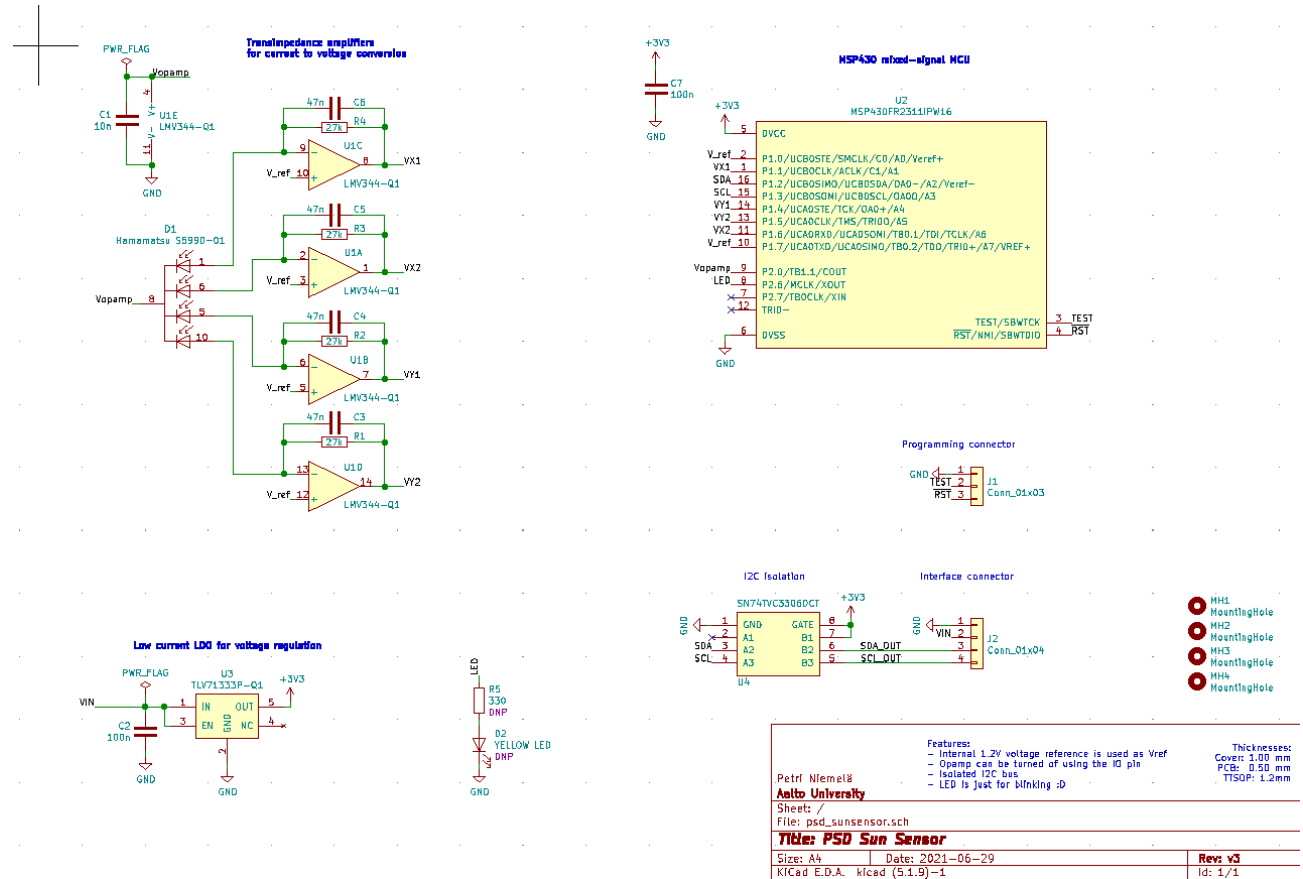
Page: 20 / 22

<http://oaji.net/articles/2017/1330-1507024153.pdf>

7 Appendices

7.1 Schematics

Version 3



7.2 Bill of Material

Refs	Qty	Manufacturer	Name	Description/Comment
U1	1	Texas Instruments	LMV344-Q1	Automotive Grade Rail-to-Rail Output CMOS Op Amp
U2	1	Texas Instruments	MSP430FR2311PW16R	16-bit Microcontrollers - MCU 16 MHz Ultra-Low-Power Microcontroller
U3	1	Texas Instruments	TLV71333P	LDO Voltage Regulators Automotive Capacitor-Free 150mA Low-Dropout (LDO) Regulator
U4	1	Texas Instruments	SN74TVC3306DCUR	Dual Voltage Clamp
C2,C7	2	Generic	100 nF 0603 SMD Capacitor	C0G and automotive grade

PSD Sun Sensor Design Document

FS1 ADCS PSD Sun Sensor Design Document

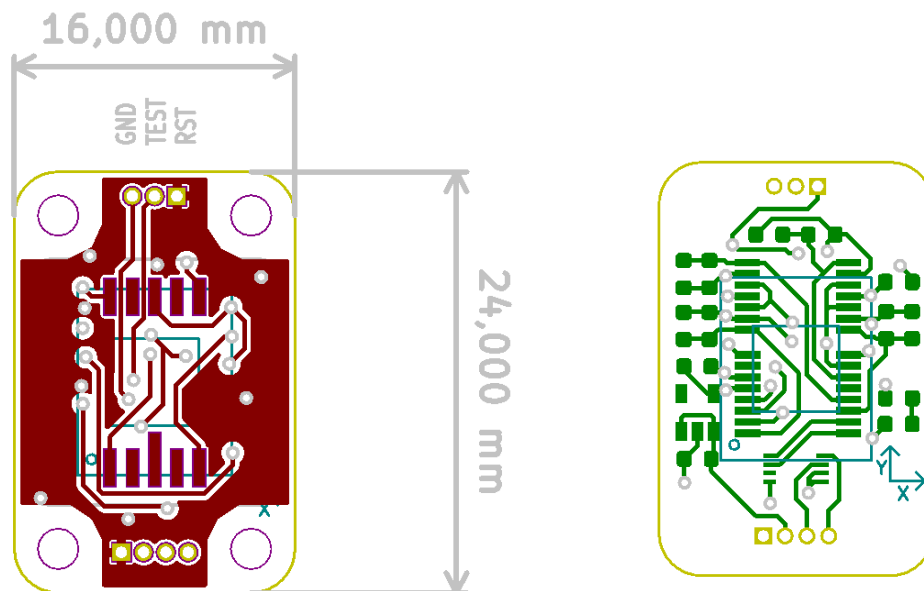
Responsible: Petri Niemelä

Version date: 2023-01-26

Page: 22 / 22

C1,C3, C4,C5, C6	5	Generic	10 nF 0603 SMD Capacitor	C0G and automotive grade
R1,R2, R3,R4	4	Generic	9k1 ohm 0603 SMD Resistor	Automotive grade
R5	1	Generic	LED current limit 0603 SMD resistor	Do not populate on FM
D2	1	Generic	Yellow 0603 SMD LED	Do not populate on FM
D1	1	Hamamatsu	S5990-01	Position Sensitive Detector (diode)
MH1, MH3	2	Generic	A4 stainless steel M2 x 4mm pan head screw	Non magnetic!
MH2, MH4	2	Generic	A4 stainless steel M2 x 2mm pan head	Non magnetic!

7.3 PCB layout



PCB front-side and back-side of hardware version 3

- Dimension: 16 mm × 24 mm
- PCB thickness: 0.5 mm